in vacuo at ca. 250 °C. The dichlorides of chromium and zinc (and occasionally nickel) were prepared from the reaction of high-purity metals (Goodfellow) with AgCl in an argon atmosphere, using a metal:AgCl ratio of approximately 10:1. The tube containing the reactants was then evacuated so that the dichloride could be sublimed away from the metal and sealed off for storage. For the synthesis of $Cr^{37}Cl_2$, isotopic $Ag^{37}Cl$ was prepared from enriched $Na^{37}Cl$ (Monsanto 95% $^{37}Cl$). $FeCl_2$ and $NiCl_2$ were prepared from the reaction of high-purity metal wire or foil with HCl (gas) (BDH 99.6%). Matrix gases were as follows: high-purity argon (BOC 99.998%), carbon monoxide (BOC research grade 99.95%), $^{13}CO$ (Amersham International 99% $^{13}C$), and $C^{18}O$ (Bureau des Isotopes Stable 97% $^{18}O$).

**Matrix Isolation Infrared Spectroscopy.** The anhydrous or sublimed materials were transferred to a conventional matrix isolation apparatus[47] equipped with a silica dome and radio frequency (in the case of $CaCl_2$) or resistive heating. Sample deposition times were typically 1 h, and the vapors were cocondensed with a large excess of matrix gas onto a CsI window held at 8-9 K by a closed cycle refrigerator (APD Cryogenics DE204SL). Sublimation temperatures for the dichlorides followed the expected trend across the series and were *approximately* as follows (°C): Ca, 900; Cr, 650; Mn, 520; Fe, 450; Co, 450; Ni, 450; Zn, 300. Infrared spectra were recorded in the region 4000-200 $cm^{-1}$ using a purged Perkin-Elmer PE983G spectrometer operating normally at a resolution of 0.65 $cm^{-1}$ and calibrated using water vapor. Spectral manipulations were carried out with a PE 3600 data station.

**Matrix Isolation X-ray Absorption Experiments.** For the EXAFS matrix isolation experiments, the techniques used[24] were similar to those described above except that (a) the central window was aluminum (Goodfellow 99.995%) and (b) deposition was monitored by observing the increase in the absorption edge (typical time 4-5 h). In order to mask fluorescence due to metal impurities in the aluminum, the window was pretreated with a thin film of krypton (for the chromium studies) or argon (for the iron studies). X-ray absorption spectra were measured in the fluorescence mode using an Ar/He-filled ion chamber (Cr, 15 Torr of Ar; Fe, 24 Torr of Ar) to monitor $I_0$ and a Tl-doped NaI crystal scintillator to monitor $I_f$. Typically, six to eight spectra were recorded and averaged.

The data were collected on station 8.1 of the SERC Daresbury Laboratory Synchrotron Radiation Source (SRS) using Si[111] or Si[220] order sorting double crystal monochromators at 50% harmonic rejection and a platinum focusing mirror. The SRS operated at 2 GeV with beam currents in the range 200-300 mA, and data were collected at the metal K-edges. Background subtraction was carried out using PAXAS[48] by fitting the preedge region to a quadratic polynomial and subtracting this function from the whole spectrum. The atomic component of the oscillatory part of the spectrum was approximated using high-order (typically six) polynomials and optimized by minimizing the chemically insignificant shells ($r < 1$ Å) in the Fourier transform. Curve fitting utilized the curved wave theory in the SERC Daresbury Laboratory EXCURVE90 program.[49] Phase shifts and backscattering factors were calculated by the usual ab initio methods[49] and found to be satisfactory without further modification.

**Acknowledgment.** We thank Miss Ingrid Fussing, Mr. Mark Keeble, and particularly Mr. A. D. Willson for preliminary work. Dr. P. Goggin provided original infrared and Raman spectra while Professor H. F. Schaefer sent us a manuscript prior to publication. We thank Professor J. Evans and Dr. W. Levason for many helpful discussions; Drs. W. Levason, J. S. Ogden, and particularly M. D. Spicer for help with the synchrotron experiments; and the Science and Engineering Research Council (U.K.) and AEA Technology, Winfrith (U.K.), for financial support. We also thank the Director of Daresbury Laboratory for experimental and computational facilities.

(47) Beattie, I. R.; Jones, P. J.; Millington, K. R.; Willson, A. D. *J. Chem. Soc., Dalton Trans.* **1988**, 2759-2762.

(48) Binsted, N. *PAXAS, Program for the Analysis of X-ray Absorption Spectra*; University of Southampton (U.K.), 1988.

(49) Gurman, S. J., Binsted, N., Ross, I. *J. Phys. C* **1984**, *17*, 143-151; **1986**, *19*, 1845-1861.

# Dehydrogenation of Ethylene and Propylene and Ethylene Polymerization Induced by $Ti^+$ in the Gas Phase

**B. C. Guo and A. W. Castleman, Jr.***

*Contribution from the Department of Chemistry, The Pennsylvania State University, University Park, Pennsylvania 16802.* *Received January 9, 1992*

**Abstract:** The chemistry of multiple-step reactions of $Ti^+$ with ethylene and propylene was examined using a SIDT-LV apparatus (selected ion drift tube with laser vaporization source) at thermal energies. Bare $Ti^+$ exhibits an active dehydrogenation reactivity toward the alkene molecules. However, the coordination of ligands on $Ti^+$ dramatically alters its dehydrogenation reactivity. For propylene, the multiple-step reactions virtually terminate at the fourth step, whereas the reactions with ethylene molecules go far beyond the fourth step. Over 20 ethylene molecules, thus far, have been observed to react with $Ti^+$, whereupon their products attach to $Ti^+$. On the basis of various experimental results, we believe that a large number of ethylene molecules attaching onto a bare $Ti^+$ at room temperature indicates that the polymerization of ethylene induced by $Ti^+$ has occurred in the gas phase and that the polymerization process follows essentially the same mechanism by which olefin polymerization catalyzed by Ziegler-Natta catalysts proceeds in the condensed phase. According to the basic concepts of Cossee's theory, we have developed a simple model to interpret the findings. The model suggests that titanacyclobutane is formed in a six-coordinated Ti(I) complex to initiate the ethylene polymerization. Then, more ethylene molecules will coordinate onto the vacant coordinating site of $Ti^+$, followed by the interposition of the coordinated ethylene from $Ti^+$ to the alkyl group. The reaction patterns are indicative of a continuing stepwise mechanism leading to the formation of a larger and larger ethylene polymer.

## 1. Introduction

One of the most exciting and far-reaching discoveries in chemistry over the past 40 years is the use of transition metal complex catalysts for alkene and diene polymerization. It was Ziegler and Natta who discovered the so-called Ziegler-Natta catalyst in the 1950's which made a revolutionary change in the modern rubber and plastics industry.[1,2] Since then, vast amounts of research in this area have been carried out by both industrial and academic scientists. The research ranges from the development of new high-activity industrial catalysts to fundamental research.[3-6] As a result, the Ziegler-Natta catalyst has been continuously upgraded to improve the commercial production of olefin polymers.

(1) Ziegler, K.; Holzkampf, E.; Breil, H.; Martin, H. *Angew. Chem.* **1955**, *67*, 541.

(2) Natta, G. *J. Polym. Sci.* **1955**, *16*, 143.

(3) *Transition metals and Organometallics as Catalysts for Olefin Polymerization*; Kaminsky, W., Sinn, H., Eds.; Springer Verlag: Berlin, 1987.

(4) *Transition Metal Catalyzed Polymerizations*; Quirk, R. P., Ed.; Cambridge University Press: Cambridge, 1988.

(5) *Catalytic Olefin Polymerization*; Keij, T., Soga, K., Eds.; Elsevier: New York, 1990.

(6) *Transition Metal Catalyzed Polymerization*; Quirk, R. P., Ed.; MMI Press: Harwood, 1983.

0002-7863/92/1514-6152$03.00/0 

Surprisingly, despite its success in commercial production, the mechanisms of the polymerization process catalyzed by Ziegler–Natta catalysts have not been as yet fully elucidated.[7] In the past 25 years, there have been a number of models and theories proposed to interpret the polymerization process.[8] Although some theoretical calculations and experimental work have provided evidence directly or indirectly supporting various models, many questions remain unanswered, and numerous findings have not as yet been explained.[9] Therefore, studies of the polymerization mechanisms remain as important research projects, and new models and theories are continuing to be developed to unravel various unsolved problems.

In the last several decades, gas-phase ion chemistry has been one of the very active research areas in chemistry.[10-12] This is due in part to expectations that ion chemistry can provide some insight into the intermediates and mechanisms of certain reactions which occur in the condensed phase, because in the gas phase, various reactions can be examined without interference from solvents (or the crystal lattice) which often hinder investigations in the condensed phase. In the late 1970's and early 1980's, a number of groups commenced study of olefin polymerization in the gas phase. They examined the reactions of several $Ti^+$ complexes with various olefin molecules using ICR techniques.[13,14] Due to the lack of numerous collisions in ICR cells and for other reasons, no olefin polymerization was observed.

In this paper, we report our recent efforts to probe olefin polymerization in the gas phase using a SIDT-LV apparatus (selected ion drift tube with laser vaporization source). The new work is motivated by recent experimental findings and calculational results which indicate that "cation-like" catalysts can have a high catalytic reactivity toward olefin polymerization.[15-17] In addition, SIDT-LV, in which the reactant ions are able to undergo thousands of collisions with the buffer and the reactant gas, offers us an effective tool for inspecting ion–molecule reactions such as a polymerization process which requires a large number of collisions between the metal ions with the buffer and reactant gases. The primary objective of the present work is to explore the possibility that the metal cation is capable of catalyzing the olefin polymerization in the gas phase. It is expected that the investigations can provide some further guide to future gas-phase investigations of the mechanisms of olefin polymerization catalyzed by Ziegler–Natta catalysts. The metal ion used to catalyze olefin polymerization in the present work is bare $Ti^+$. Ethylene and propylene, which are the two simplest and most widely used olefin molecules, are chosen as the reactant molecules.

## 2. Experimental Section

The apparatus used in the work is a SIDT-LV (selected ion drift tube with laser vaporization source), which is designed to be utilized in studies of ion–molecule reactions at thermal energies. The details of the apparatus, including procedures to produce metal ions and detect products, have been published previously.[18,19] Only a brief description of the operational techniques and the conditions used in the present work are given. $Ti^+$ is produced by the pulsed laser vaporization source.[20] Other ion species such as $TiO^+$ and cluster ions, besides $Ti^+$, are also produced from the source. After exiting the source and passing through a skimmer, the ion species are focused into the first quadrupole mass spectrometer where in the present study only $Ti^+$ is subjected to mass selection. Then, the selected ions are refocused into an ion beam by the second group ion lens and injected into the drift tube reactor through a 1.0 mm diameter orifice in the entrance plate. The drift tube reactor, where the reactions occur between the selected ions and the reactant gases, is comprised of a main cylindrical copper tube (9.0 cm i.d. by 2.9 cm long) and a pair of stainless steel plates which serve as the entrance and exit plates. The reactor pressure measured by a capacitance manometer is maintained at about 0.7 Torr with He as the buffer gas. A drift voltage is applied across the entrance and exit plates to drift both the reactant and product ions toward the exit plate. After travelling across the drift tube, a small fraction of the reactant and product ions diffuse through a 1.0-mm orifice of the exit plate into the high-vacuum chamber. There, the ions are focused into the second quadrupole mass spectrometer affixed with a Channeltron electron multiplier tube where they are mass analyzed and detected.

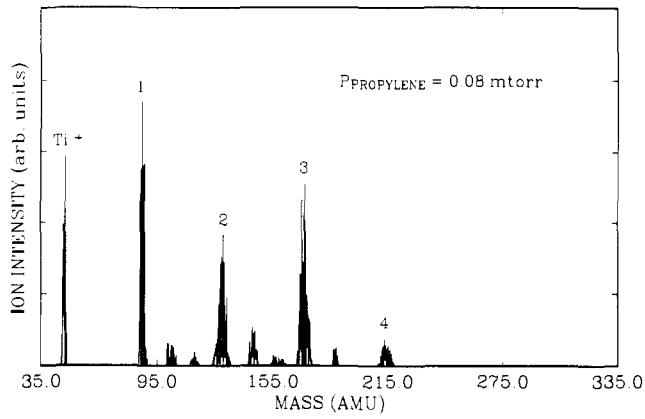


**Figure 1.** Product distribution acquired from the reactions of $Ti^+$ with propylene molecules.

The experiments are conducted at room temperature. Normally, an injected ion will remain in the drift tube reactor for more than 500 μs before exiting from the reactor, and its products can stay even longer. Since the metal ion and its products undergo thousands of collisions with the buffer gas He and the reactant ethylene or propylene, the reactions occurring in the reactor are expected to be the room-temperature thermal reactions. The reactant gases used here are polymer grade purity (ethylene, 99.5%; propylene, 99.0%).

## 3. Results

**3.1. The Propylene and Ethylene Dehydrogenation.** Titanium has five major isotopes, which could lead to the overlap of the peaks corresponding to the products formed from different isotopes. In order to eliminate the potential interference problem, we set the resolution of the first quadrupole mass spectrometer as high as possible so that only the most abundant isotope, $^{48}Ti^+$, is selected and then injected into the reactor.

Figure 1, which covers the mass range from 35 to 335 amu, shows the mass spectrum acquired from the reactions of $Ti^+$ with the propylene molecule at a propylene partial pressure of 0.08 mTorr. The labeled product peaks appearing in the mass spectrum correspond to the products generated from the first four reaction steps. The unlabeled peaks may come from the impurities in the propylene sample, although it is likely that the unlabeled peaks could also be decomposition products resulting from $Ti^+$ breaking the C–C bond of propylene. Since we do not know the origin of the peaks, no further discussion of them is given in this paper. The mass spectra obtained under high-resolution conditions reveal that many of the labeled product peaks contain several subpeaks, which indicates that several pathways occur in the reaction steps. From the high-resolution mass spectra, we are able to determine the major products formed from each of the first four steps. The

(7) Pino, P.; Mulhaupt, R. *Angew. Chem., Int. Ed. Engl.* **1980**, *19*, 857.
(8) Ledwith, A.; Sherrington, D. C. In *Reactivity, Mechanism and Structure in Polymer Chemistry*; Jenkins, A. D., Ledwith, A., Eds.; John Wiley & Sons: New York, 1974; pp 384–427.
(9) Ystenes, M. *J. Catal.* **1991**, *129*, 383 and references therein.
(10) Allison, J. *Inorg. Chem.* **1986**, *34*, 627 and references therein.
(11) Martinho, J. A.; Beauchamp, J. L. *Chem. Rev.* **1990**, *90*, 629.
(12) Armentrout, P. B. In *Gas Phase Inorganic Chemistry*; Russell, D. H., Ed.; Plenum: New York, 1989.
(13) (a) Allison, J.; Ridge, D. P. *J. Am. Chem. Soc.* **1977**, *99*, 33. (b) Allison, J.; Ridge, D. P. *J. Am. Chem. Soc.* **1978**, *100*, 163. (c) Kinser, R.; Allison, J.; Dietz, T. G.; de Angelis, M.; Ridge, D. P. *J. Am. Chem. Soc.* **1978**, *100*, 2706.
(14) Uppal, J. S.; Johnson, D. E.; Stanley, R. H. *J. Am. Chem. Soc.* **1981**, *103*, 508.
(15) Yang, X.; Stern, C. L.; Marks, T. J. *J. Am. Chem. Soc.* **1991**, *113*, 3623 and references therein.
(16) Jolly, C. A.; Marynick, D. S. *J. Am. Chem. Soc.* **1989**, *111*, 7968.
(17) Lauher, J. W.; Hoffmann, R. J. *J. Am. Chem. Soc.* **1976**, *98*, 1729.
(18) Guo, B. C.; Kern, K. P.; Castleman, A. W., Jr. Chemistry and Kinetics of Reactions of $Ti^+$ with $H_2O$, $NH_3$, $CH_3OH$, $C_2H_4$, and $C_3H_6$ at thermal energies. *J. Phys. Chem.*, in press.
(19) Guo, B. C.; Kerns, K. P.; Castleman, A. W., Jr. Chemistry and Kinetics of Size Selected Cobalt Cation Clusters at Thermal Energies: 1. Reactions with CO. *J. Chem. Phys.*, in press.
(20) Tietz, T. G.; Duncan, M. A.; Powers, D. E.; Smalley, R. E. *J. Chem. Phys.* **1981**, *74*, 6511.

**Table I.** The Stoichiometry of the Major Products Formed from the Multiple-Step Reactions of $Ti^+$ with Propylene and Ethylene Molecules at Thermal Energies[a]

| step no. | propylene | ethylene |
|---|---|---|
| 1 | $Ti(B)^+$ | $Ti(A)^+$ |
| 2 | $Ti(B)_2^+$ (VH) | $Ti(A)(E)^+$ (VH) |
| | $Ti(B)(T)^+$ (L) | $Ti(A)_2^+$ (VL) |
| | $Ti(B)(P)^+$ (M) | |
| 3 | $Ti(B)_2(P)^+$ (VH) | $Ti(A)(E)_2^+$ (VH) |
| | $Ti(B)(T)(P)^+$ (L) | $Ti(A)_2(E)^+$ (L) |
| | $Ti(B)(P)_2^+$ (M) | $Ti(A)_3^+$ (L) |
| 4 | $Ti(B)_2(P)_2^+$ (H) | $Ti(A)(E)_3^+$ (VH) |
| | $Ti(B)(T)(P)_2^+$ (M) | $Ti(A)_2(E)_2^+$ (VH) |
| | $Ti(B)(P)_3^+$ (M) | $Ti(A)_3(E)^+$ (L) |
| | | $Ti(A)_4^+$ (L) |
| 5 | | $Ti(A)(E)_4^+$ (VH) |
| | | $Ti(A)_2(E)_3^+$ (VH) |
| | | $Ti(A)_3(E)_2^+$ (L) |
| | | $Ti(A)_4(E)^+$ (L) |
| 6 | | $Ti(A)(E)_5^+$ (VH) |
| | | $Ti(A)_2(E)_4^+$ (VH) |
| | | $Ti(A)_3(E)_3^+$ (M) |
| | | $Ti(A)_4(E)_2^+$ (H) |
| 7 | | $Ti(A)(E)_6^+$ (VH) |
| | | $Ti(A)_2(E)_5^+$ (VH) |
| | | $Ti(A)_3(E)_4^+$ (L) |
| | | $Ti(A)_4(E)_3^+$ (L) |
| 8 | | $Ti(A)(E)_7^+$ (VH) |
| | | $Ti(A)_2(E)_6^+$ (VH) |
| | | $Ti(A)_3(E)_5^+$ (L) |

[a] Note: A represents $C_2H_2$, B $C_3H_4$, T $C_3H_2$, E ethylene, and P propylene. VH, H, M, L, and VL represent the relative abundance of the products from each of the listed reactions. The explanation of the symbols is given in the text.

stoichiometric formulas of the products are listed in Table I, along with the measured relative product abundance which is labeled by VH, H, M, L, and VL. VH designates that the product has very high abundance, H high abundance, M medium abundance, L low abundance, and VL very low abundance. The measurement of the absolute product abundance is limited by several factors, especially by the existence of further sequential reactions. Hence, we list in the table the relative product abundances instead of the absolute ones. For the sake of simplification, in Table I, A is used to represent product $C_2H_2$ produced by loss of one hydrogen molecule from an ethylene molecule, B and T stand for $C_3H_4$ and $C_3H_2$ generated from loss of one and two hydrogen molecules, respectively, from a propylene molecule, and P and E stand for propylene and ethylene. In the remaining part of the paper, these symbols will denote the same molecules unless a specific note is given.

Generally, the reactions of $Ti^+$ with propylene molecules involve two classes of reaction pathways, namely dehydrogenation and association. For the primary reaction, our previous work[18] indicated that $Ti^+$ displays an extraordinary degree of dehydrogenation reactivity toward propylene according to reaction 1.

$$Ti^+ + CH_3CHCH_2 = Ti(B)^+ + H_2 \quad (1)$$

As for the second step reaction, in addition to reaction 4, which represents the dehydrogenation process with loss of one hydrogen molecule from propylene, two more reaction pathways as expressed by reactions 2 and 3 are observed due to the coordination of a ligand B onto $Ti^+$. Reaction 2 represents the process resulting in loss of two hydrogen molecules from a propylene molecule, while reaction 3 represents the association of a propylene molecule onto $Ti^+$. To obtain a reliable product abundance, the partial pressure

$$Ti(B)^+ + CH_3CHCH_2 = Ti(B)(T)^+ + 2H_2 \quad (2)$$

$$= Ti(B)(P)^+ \quad (3)$$

$$= Ti(B)_2^+ + H_2 \quad (4)$$

of propylene was kept as low as possible to prevent the products formed from reactions 2–4 from undergoing further reactions with propylene molecules. The same procedures are also used to obtain the relative product abundances from the other reaction steps.

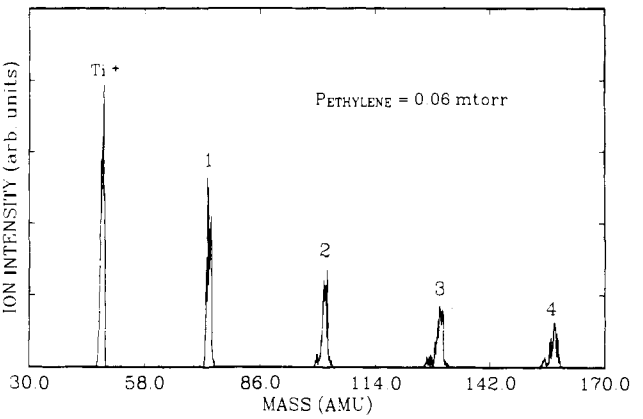


**Figure 2.** Product distribution acquired from the first four reaction steps of $Ti^+$ with ethylene molecules.

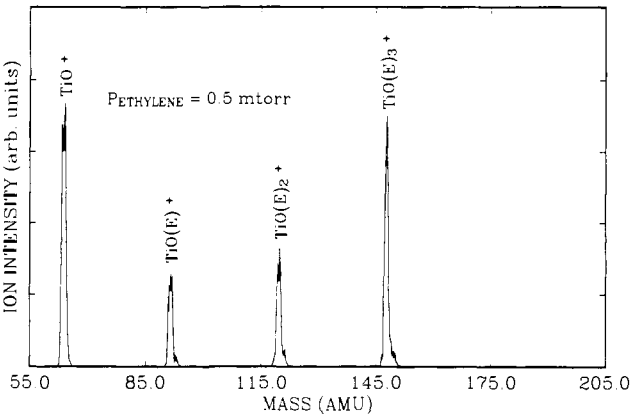


**Figure 3.** Product distribution acquired from the reactions of $TiO^+$ with ethylene molecules.

It is observed that the product distributions of the third and the fourth steps are very similar to that of the second reaction step. This suggests that the association pathways are dominant in the third and the fourth reaction steps.

Figure 2 is the typical mass spectrum in the range from 30 to 170 amu resulting from the first four reaction steps of $Ti^+$ with ethylene at an ethylene partial pressure of 0.06 mTorr. The peaks labeled by numbers correspond to the product of the $n$th reaction step. Since some of the results of these reactions have been reported previously,[21] only the products and their relative abundances are listed in Table I. In general, association and dehydrogenation with loss of one hydrogen molecule are the two principal reaction pathways in the first four reaction steps of $Ti^+$ with ethylene molecules.

For purposes of comparison, we also studied the reactions of $TiO^+$ with ethylene. Figure 3 is a product distribution from the reactions of $TiO^+$ with ethylene at 0.2 mTorr. It is apparent that all three reaction steps lead to a coordination of one ethylene molecule onto $TiO(E)_{n-1}^+$ according to reaction 5. Interestingly,

$$TiO(E)_{n-1}^+ + E = TiO(E)_n^+ \qquad n = 1\text{–}3 \quad (5)$$

further increase in the partial pressure of ethylene does not bring about clustering more ethylene molecules around $TiO^+$, which suggests that the reactions terminate at the $n = 3$ step.

**3.2. Further Reaction Steps of $Ti^+$ with Ethylene.** We conducted studies in which the partial pressure of propylene was increased up to about 0.1 Torr to see whether $Ti^+$ would continuously react with propylene beyond the fourth step reaction. But, surprisingly, except that more and more products from the first three reaction steps are observed to become converted into the products of the fourth step, no further reactions were found

(21) Guo, B. C.; Castleman, A. W., Jr. Effect of Ligands on the Reactivity of $Ti^+$ and $V^+$ Toward Breaking C–H Bonds of Ethylene. *Int. J. Mass Spectrom. Ion Proc.* **1992**, *113*, R1–R5.

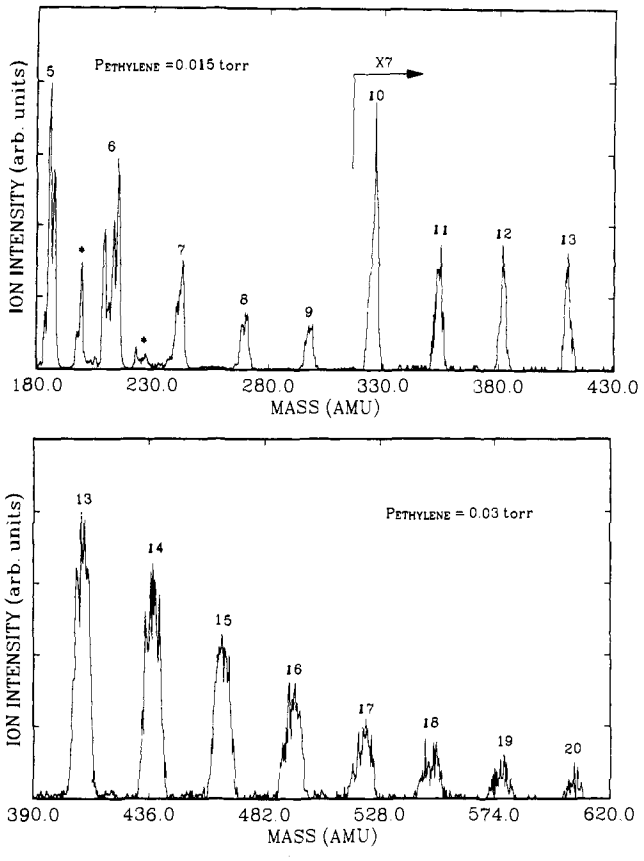


**Figure 4.** (a, top) Product distribution acquired from the 5th to 13th reaction steps of $Ti^+$ with ethylene molecules. (b, bottom) Product distribution obtained from the 13th to 20th reaction steps of $Ti^+$ with ethylene molecules.

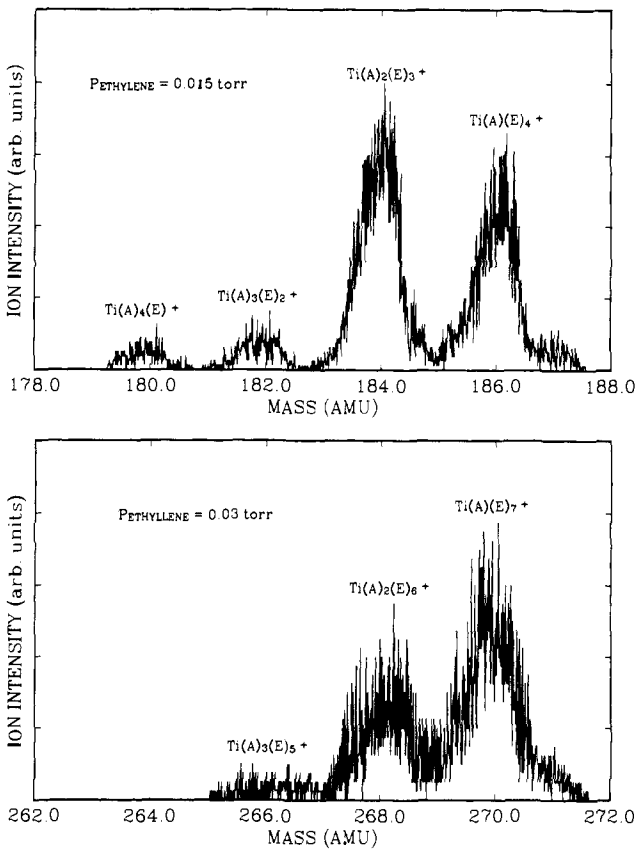


**Figure 5.** (a, top) High resolution mass spectrum of the product distribution from the fifth step reaction. (b, bottom) High resolution mass spectrum of the product distribution from the eighth step reaction.

at propylene pressures ranging up to 0.1 Torr.

As for ethylene, the story is completely different. $Ti^+$ reacts continuously with ethylene molecules far beyond the four reaction steps. Thus far, $Ti^+$ is observed to react with as many as 20 ethylene molecules. Meanwhile, the products from the further sequential reactions are also bound onto $Ti^+$ as are the products from the first four reaction steps. Figure 4a shows the mass spectrum from 180 to 430 amu, which is acquired as a result of multiple-step sequential reactions of $Ti^+$ with ethylene molecules at an ethylene partial pressure of 0.015 Torr; and Figure 4b shows the mass range from 390 to 620 amu obtained at an ethylene partial pressure of 0.03 Torr. The peaks in Figure 4 labeled by a number correspond to the products formed from the *n*th reaction step, respectively. The peaks labeled by an asterisk, and observable in the low mass range, may result from impurities in the ethylene gas.

As in the case of the first four reaction steps, by setting the second quadrupole mass spectrometer on the high-resolution model, we are able to determine the components contained in the peaks labeled 5–8. For instance, spectra a and b in Figure 5, are the high-resolution mass spectra of peaks 5 and 8 shown in Figure 4a. It appears that the peaks contain several major subpeaks and that the mass spacing between the major subpeaks in the spectra is 2 amu. The stoichiometric composition of the products from those reaction steps is also listed in Table I. As can be seen from Table I, the fifth to the seventh reaction steps produce four major products, whereas only three main products are observed in the eighth step of the reaction.

Since the signal levels for the larger molecule are very weak and setting the quadrupole mass spectrometer to high-resolution conditions dramatically decreases its efficiency in transmitting high-mass ions, the resolution cannot be set high enough to resolve peaks 9–20 appearing in spectra a and b in Figure 4. As a result, we could not determine the stoichiometry of the products from the 9th to the 20th steps of the reactions. However, we have made efforts to set the resolution of the second quadrupole mass spectrometer as high as possible to assist in determining the mass of those products. The mass spacing between the central position of the neighboring peaks is observed to be even and equal to one mass unit of the ethylene molecule. From the width of the peaks in the high-resolution mass spectra, we can estimate that the accuracy of the position determined for each peak in the mass spectrum is about 2 amu. Hence, we are very certain that the product pattern corresponding to the peaks from the 9th to the 20th steps of the reactions is similar to the product pattern from the 8th reaction step. That is, each of these reaction steps leads to the bonding of one more ethylene molecule to $Ti^+$.

We have also examined the relationship of the signal intensities of the peaks to the partial pressure of the ethylene in order to probe the relative reaction rate for each of the reactions. At a very low ethylene partial pressure, the products formed from the first four steps of the reactions are dominant in the mass spectra. With an increase of the partial pressure of ethylene, the peaks corresponding to the first three reactions quickly vanish from the mass spectrum, while the peaks for the fifth and the sixth reaction steps begin to grow; eventually, the intensities of the two peaks become comparable to that for the fourth reaction step at relatively high partial pressures of ethylene. As illustrated in Figure 4a,b, with further increase of the partial pressure of ethylene, the peaks corresponding to the 7th to the 20th steps of the reactions gradually appear in the mass spectra, but the signal intensities of these peaks are observed to be lower than those for the 5th and the 6th steps of the reactions and to decrease monotonically even at an ethylene partial pressure of 0.1 Torr. It is apparent that the reactions can be classified into three categories according to the reaction rate. The first four reaction steps are very fast ($k = 3.5 \times 10^{-10}$ cm$^3$/s for the first reaction step);[18] the reaction rates for the fifth and the sixth steps are relatively slow, and their rates are estimated to be slower than those for the first four steps by one order of magnitude. Starting from the 7th step, the reactions become extremely slow, and their reaction rates are probably slower than those for the first four steps by more than two orders of magnitude.

## 4. Discussion

**4.1. Dehydrogenation Reactions.** As with other reactants containing H atoms,[22,23] bare $Ti^+$ demonstrates an active dehy-

drogenation reactivity toward ethylene and propylene as well. Nevertheless, the coordination of ligands onto $Ti^+$ can significantly change its dehydrogenation reactivity. In the case of reactions with ethylene, the coordination of an acetylene molecule onto $Ti^+$ leads to a great reduction in the dehydrogenation reactivity of $Ti^+$. Interestingly, adding an oxygen atom instead of acetylene or ethylene molecule onto $Ti^+$ completely destroys the dehydrogenation reactivity of $Ti^+$ toward ethylene. In a previous note on this subject,[21] we reported that the extent to which coordinated ligands influence the dehydrogenation reactivity of metal ions depends on the number of ligands and types of metal ions. The difference in dehydrogenation reactivity of $Ti^+$ resulting from coordinating an oxygen atom and an acetylene molecule suggests that the extent to which the coordinated ligands alter the dehydrogenation reactivity of $Ti^+$ may also depend on the type of ligands.

As for the reactions of $Ti^+$ with propylene molecules, we find that coordinating a ligand of $C_3H_4$ onto $Ti^+$ leads to an unusual reaction pattern. As mentioned above, the only reaction pathway corresponding to the primary reaction step with propylene is a dehydrogenation process with loss of one hydrogen molecule according to reaction 1. However, it is found that the coordination of one $C_3H_4$ onto $Ti^+$ opens two additional new reaction channels. One of these involves the association of a propylene molecule onto $Ti(B)^+$ as expressed by reaction 3, which suggests that the coordination of B has led to a reduction in the dehydrogenation reactivity of $Ti^+$. But, surprisingly, another new pathway according to reaction 2 is able to produce the product with loss of two hydrogen molecules, which, by contrast, indicates that the dehydrogenation activity of $Ti^+$ might be enhanced by coordinating B. Obviously, reactions 2 and 3 show a comparison of the effects of the coordinated B on the dehydrogenation reactivity of $Ti^+$.

There are several possibilities to account for the effect of the coordinated ligands onto the dehydrogenation reactivity of transition metal ions. For instance, the coordination of ligands onto a metal ion may well change the electronic structure of the ion. The effect of ligands may depend on the variation in the electronic structure of the metal ion. Some ligands could lead to an electronic structure enhancing the reactivity, while others may result in a structure that leads to a reduction in the reactivity. On the other hand, it may be argued that the ligands could couple with each other to form a new ligand, thereby leading to an enhancement or diminution in the dehydrogenation reactivity of metal ions. Of course, these discussions are purely speculative. More experimental work and calculational investigations are needed to elucidate the real origin of the effects due to the coordination of ligands on the reactivities of transition metal systems.

**4.2. Ethylene Polymerization Catalyzed by $Ti^+$.** The most fascinating result coming from the present work is the finding that as many as 20 ethylene molecules can react with a bare $Ti^+$ and their products remain bonded onto the ion. As pointed out in our previous communication,[24] there are two potential processes to account for a large number of ethylene molecules being bound to a bare $Ti^+$. One would involve a simple clustering of ethylene molecules onto $Ti^+$ to form a large ion–molecule complex in which the ligands and $Ti^+$ are bound together by pure electrostatic interactions, whereas another possibility is that the ligand molecules react with each other, induced by $Ti^+$, to form a large ethylene polymer which is bound onto $Ti^+$. However, considering the facts that the experiments are not performed at low temperature nor high pressure and ethylene has no dipole moment, it is virtually impossible that over 20 ethylene molecules would be able to cluster onto bare $Ti^+$. In fact, this argument is strongly supported by many test experiments made on this point.

If electrostatic interactions were responsible for the processes that lead to the formation of large ion–molecule complexes, similar interactions would be expected to occur in reactions of other transition metal ions with ethylene molecules as well. To investigate this, we performed studies of the reactions of other transition metal ions such as $V^+$, $Zr^+$, $Ta^+$,[25] and $Ag^+$[26] to explore the possibility that a large number of ethylene molecules could cluster onto a bare metal ion under experimental conditions similar to those used in the present work. It is found that the maximum number of ethylene molecules that can attach onto those metal ions is less than 8! This result, therefore, clearly indicates that simple clustering reactions could not lead to the association of as many as 20 ethylene molecules onto a bare $Ti^+$ at room temperature! Additionally, the results from the work on the reactions of $TiO^+$ with ethylene, which results in only three ethylenes bonding onto $TiO^+$, also support the above argument.

Therefore, it is apparent that the only possibility to account for the experimental findings is that ethylene polymerization induced by $Ti^+$ occurs and leads to the formation of a large polymer which remains bound onto $Ti^+$. Now the question which needs to be addressed is how the ethylene molecules become polymerized by $Ti^+$ in the gas phase. We discuss this point in the remainder of this subsection.

Since $Ti^+$ is a cation, one may at first consider that the cationic polymerization reaction is a potential process. Cationic polymerization of olefin molecules is a major polymerization process in the condensed phase, and its mechanism and reactivity have been well characteized in the literature.[27-30] The polymerization is considered to be initiated by charge transfer from the cationic species to the olefin molecule. However, as for the current case, since the IP of ethylene (10.5 eV) is much higher than the first IP (6.8 eV) of elemental titanium,[31] it is essentially impossible to transfer a positive charge from $Ti^+$ to ethylene at thermal energies. (Note: Since the experiment was conducted at thermal energies, the reactions observed to occur in the drift tube reactor must be exothermic.) Hence, the traditional cationic polymerization mechanism cannot be applied to explain the present polymerization reactions.

Titanium compounds are the key components in Ziegler–Natta catalysts, and most of the current theories have regarded titanium as the active center of Ziegler–Natta catalysts.[3-6] Moreover, there have been reports that the cation-like Ziegler–Natta catalysts are highly active toward olefin polymerization.[15-17] Therefore, we tend to argue that the gas-phase ethylene polymerization process observed in the work is somewhat similar to olefin polymerization reactions in the condensed phase catalyzed by a typical Ziegler–Natta catalyst. The best-known mechanism to account for olefin polymerization was proposed by Cossee more than 25 years ago.[32] Although there have also been a large number of the revised theories, their basic concepts are similar to Cossee's mechanism.[33-35] In general, Cossee's theory states that the active site is a transition metal having an overall octahedral configuration in which one position is vacant due to a missing ligand. This model provides a transition metal–alkyl $\sigma$-bond and the facility for coordination of monomer molecules to the transition element. Propagation of polymerization is assumed to be the interposition of the coordinated olefin molecule between the transition metal and the alkyl group. On the basis of Cossee's ideas, we have

(22) Tonkyn, R.; Ronan, M.; Weisshaar, J. C. *J. Phys. Chem.* **1988**, *92*, 92.

(23) Tolbert, M. A.; Beauchamp, J. L. *J. Am. Chem. Soc.* **1986**, *108*, 7509.

(24) Guo, B. C.; Castleman, A. W., Jr. Evidence for the Polymerization of Ethylene Catalyzed by $Ti^+$ in the Gas Phase. *J. Am. Soc. Mass Spectrom.* **1992**, *3*, 464.

(25) Guo, B. C.; Castleman, A. W., Jr. Chemistry of Multiple-step Reactions of $V^+$, $Zr^+$, and $Ta^+$ with $C_2H_4$. To be submitted for publication.

(26) Guo, B. C.; Castleman, A. W., Jr. *Chem. Phys. Lett.* **1991**, *181*, 16.

(27) Ledwith, A.; Sherrington, D. C. In *Reactivity, Mechanism and Structure in Polymer Chemistry*; Jenkins, A. D., Ledwith, A., Eds.; John Wiley & Sons: New York, 1974; pp 244–305.

(28) *The Chemistry of Cationic Polymerization*; Plesch, P. M., Ed.; Pergamon Press: New York, 1963.

(29) Pepper, D. C. *European Polym.* **1965**, *1*, 11.

(30) Zlamal, Z. In *Kinetics and Mechanism of Polymerization, Vinyl Polymerization*; Ham, G. E., Ed.; Marcel Press: New York, 1969; Vol. 1, Part II, p 231.

(31) *Handbook of Chemistry and Physics*; 65th ed.; CRC Press: Boca Raton, 1984.

(32) Cossee, P. J. *J. Catal.* **1964**, *3*, 80.

(33) Rodriguez, L. A. M.; van Looy, H. M. *J. Polym. Sci. A1* **1966**, *4*, 1951, 1971.

(34) Arlman, E. J.; Cossee, P. J. *J. Catal.* **1964**, *3*, 99.

(35) Boor Jun, J. In *Macromol. Reviews*; Interscience: New York, 1967; Vol. 2, pp 115–261.

**Scheme I**

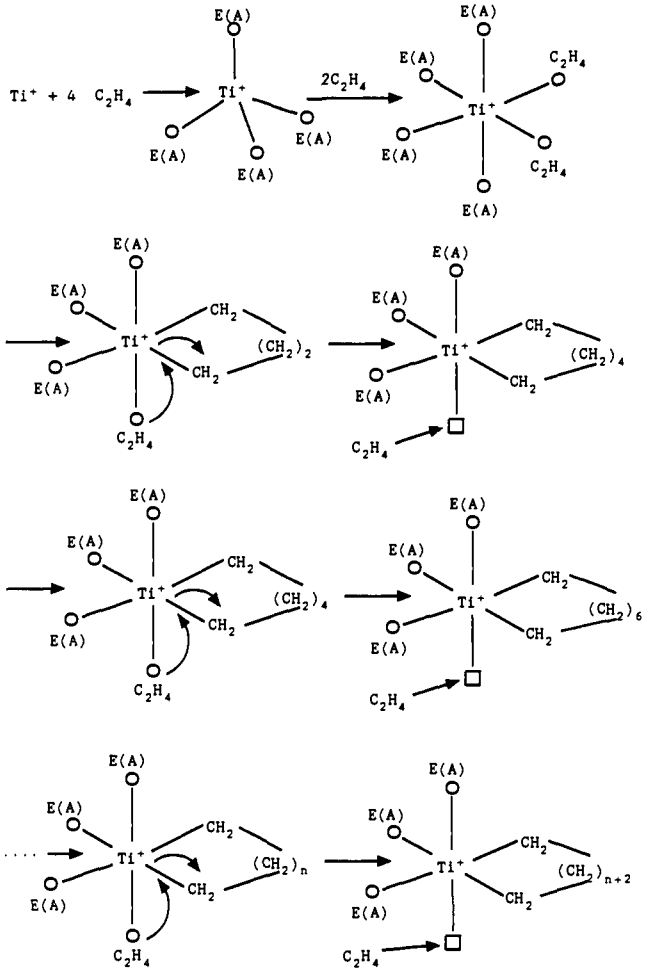

developed a simple mechanism accounting for the gas-phase ethylene polymerization process induced by $Ti^+$. The mechanism is displayed in Scheme I.

The mechanism assumes that the first four reaction steps are ion–molecule reactions which produce either dehydrogenation or association products. Therefore, the four reaction steps are observed to be fast reactions. The four-ligand-coordinated $Ti^+$ complex is assumed to have a tetrahedral structure. When the fifth and sixth ligands approach the $Ti^+$, they need to break the 4-fold symmetry of the ion complex to form a six-ligand coordinated complex with an octahedral structure as shown in Scheme I. As a result, their reaction rates become relatively shower compared to those of the first four reactions. (Note: It is also possible that the four-coordinated ligands could lead to a steric hinderance which would make further coordination of the ligands difficult and thereby reduces the reaction rates of the fifth and the sixth steps.

The next two steps are the most critical in the mechanism. Cossee's model requires a transition metal–alkyl $\sigma$-bond. As can be seen from above section, the products with an even number of hydrogen atoms are dominant in the first eight step reactions, and the products from the further sequential reactions are expected to follow the same pattern.[36] Obviously, the reactions could not produce a single metal–alkyl $\sigma$-bond because it needs an odd number of hydrogen atoms. In order to fulfill the requirements of the Cossee model, we propose the formation of a titanacyclobutane which has two Ti–alkyl $\sigma$-bonds. This assumption relies on some recent findings in organometallic chemistry. There have been a number of reports that, in the condensed phase, many metal complexes are able to catalyze two olefin molecules into a metal–cycloalkane.[37-39] Thereupon, it would not be surprising that the Ti(I) complex is also able to react with two ethylene molecules to form a titanacyclobutane ion complex. Following this step, an ethylene molecule coordinated onto $Ti^+$ will undergo the interposition from the titanium ion to the alkyl group and create one vacant position for further coordination of ethylene molecules. As shown in Scheme I, starting from the seventh ethylene molecule, the reactions of $Ti^+$ with ethylene involve only the coordination of an ethylene molecule onto $Ti^+$, and thereafter ethylene inserts into one of the metal–alkyl $\sigma$-bonds to form a larger titanacycloalkane. The reaction patterns keep expanding to form a larger and larger ethylene polymer.

As pointed out in the above section, the reaction rates for the 7th to the 20th steps are observed to decrease monotonically with the number of the reaction step, and their rates are much slower than the rates for the fifth and the sixth reaction steps. This finding is also explainable in light of the proposed mechanisms. Starting from coordinating the seventh ethylene molecule, there is a large titanacycloalkane on $Ti^+$ which would create a block to the path of the ethylene molecule toward the vacant coordination position of $Ti^+$. Moreover, the size of titanacycloalkane increases with the number of the adding ethylene molecules; thereby, it will become more and more difficult for ethylene molecules to occupy the vacant position. Thus, the reactions would be expected to have a much slower rate than those for the early reaction steps, and their reaction rates would decrease monotonically due to the blocking effect.

As can be seen from Table I, one of the products with a low abundance produced from the seventh reaction step is $Ti(A)_4(E)_3^+$. Obviously, the formation of the product from the association of one ethylene molecule onto $Ti(A)_4(E)_2^+$ cannot be explained by the above mechanism, because the above mechanism needs at least three ethylene molecules in the six-ligand-coordinated $Ti^+$ to trigger the seventh step of the polymerization process. Therefore, instead of the formation of a titanacyclobutane, one coordinatd acetylene and one ethylene molecule may undergo reaction with $Ti^+$ to form a titanacyclobutene and initiate the ethylene polymerization. But, interestingly, no product corresponding to the addition of one more ethylene molecule onto $Ti(A)_4(E)_3^+$ has been observed from the eighth reaction step, at least not within our current detection sensitivity. The result might suggest that the formation of a titancyclobutene instead of titanacyclobutane reduces the polymerization activity of $Ti^+$.

**4.3. Further Discussion.** Apparently the proposed polymerization mechanism shown in Scheme I enables an explanation of most of the results obtained from the present work. Yet, we would like to consider other reaction mechanisms. First, the idea that the titanacyclobutane is formed in the six-ligand-coordinated $Ti^+$ is quite speculative. It is very possible that the formation process occurs at an earlier stage of the coordination reactions.

It may also be argued that ethylene molecules might react with each other to form several large hydrocarbon molecules which become bound onto $Ti^+$. $Ti^+$ has six coordination sites, and the maximum number of hydrocarbons that could be formed on $Ti^+$ should be three, that is, every two of the six coordinated ligands react with each other to form a total of three hydrocarbons. However, since the formed hydrocarbons (each of them will occupy two sites just as in the case of titanacyclobutane) occupy every coordination site, even the seventh ethylene molecule could not get close to $Ti^+$ and react with the hydrocarbons to produce a larger hydrocarbon molecule. Therefore, the argument is still unable to explain the experimental evidence that more than 20 ethylene molecules can attach onto $Ti^+$.

In principle, two titanacyclobutanes which reside on four of the six coordination sites could be formed on the six-ligand-co-

(36) As seen from Figure 5a,b, there is a minor peak which is one mass unit away from the most left-side major peak. The peak is very weak and overlaps partially with the major peak. Since we do not know the origin of the peak, we do not include it in the major product distribution listed in Table I.

(37) Sen, A. *Acc. Chem. Res.* **1988**, *21*, 421.

(38) Sen, A.; Lai, T. W.; Thomas, R. R. *J. Organomet. Chem.* **1988**, *358*, 567.

(39) Jiang, Z. Z. Ph.D. Dissertation, The Pennsylvania State University, 1990.

ordinated Ti(I) complex, and the remaining two sites could serve as the vacant ones for the further coordination and insertion of ethylene molecules. As a result, one may argue that two ethylene polymers could be formed through a mechanism similar to the one shown in Scheme I. However, considering the fact that the existence of two large titanacycloalkanes would create an overcrowded sterically hindered environment around $Ti^+$ which could completely obstruct the path of other ethylene molecules to $Ti^+$ and thereby prevent them from approaching $Ti^+$, we do not think that the chance to form two large ethylene polymers would be higher than that to form one ethylene polymer. The results from the reactions with propylene molecules may provide a good example to illustrate the consequence of the steric hinderance. As discussed above, the reactions with propylene terminate at the $n = 4$ step, and no propylene molecules are able to occupy the vacant fifth and the sixth coordination sites, regardless of the partial pressure of propylene in the drift tube reactor. This suggests that the four ligands which contain as few as three carbon atoms can create a large enough hindrance of the path to the sites and thereby prevent the fifth and the sixth propylene molecules from approaching $Ti^+$.

The blocking effect of the large size ligands might be one of the reasons that a bare $Ti^+$ could not induce propylene polymerization in the gas phase. The active center in Cossee's mechanism is a transition metal having an overall octahedral configuration with one missing vacant site. The steric hinderance prevents Ti(I) complexes from having an octahedral structure in the case of propylene as the reactant gas. Consequently, a Ti(I) complex without an octahedral structure would not display catalytic activity toward propylene polymerization. On the other hand, Cossee's model requires a metal–alkyl $\sigma$-bond to initiate the olefin polymerization process. In the case of ethylene, we set forth the formation of a titanacyclobutane to provide the metal–alkyl $\sigma$-bond. However, the existence of the methyl group in propylene may greatly reduce the reaction rate of two propylene molecules with $Ti^+$ to form a titanacycloalkane, thereby, the reaction may not occur within the time scale in which $Ti^+$ stays in the reactor.

Apparently the ligands coordinated onto $Ti^+$ have a great impact on ethylene polymerization. For example, the reactions of $TiO^+$ with ethylene indicate that a coordination of an oxygen atom onto $Ti^+$ will completely destroy its catalytic activity toward ethylene polymerization. We have performed an experiment to inspect the copolymerization of ethylene and propylene induced by $Ti^+$.[40] The results from the work show that the presence of propylene can dramatically reduce the rate of ethylene polymerization. In the condensed phase, olefin polymerization processes ranging from the catalytic activity of Ziegler–Natta catalysts to the structure and distribution of polymer products are also observed to depend strongly on the crystal environment in heterogeneous catalysis and the nature of the ligand in homogeneous catalysis.[3-6]

Although the results from the present work are preliminary, they have led to the first evidence that a bare $Ti^+$ is capable of catalyzing olefin polymerization in the gas phase. This work has shown that the nature of the ligands coordinated on $Ti^+$ can have a great impact on the olefin polymerization. It would be of great significance to understand what kind of ligands could enhance the gas-phase olefin polymerization rate, because the work could provide some insight into the olefin polymerization mechanism, as well as a valuable hint for the selection of the ligands used in Ziegler–Natta catalysts. In addition, a collision-induced dissociation experiment would be very valuable because it could provide some insight into the bond structure of $Ti^+$ to the ethylene polymer, thereby revealing the existence of metal–alkyl $\sigma$-bonds. Certainly the work would enable one to further examine the olefin polymerization process catalyzed by Ziegler–Natta catalysts. We plan to commence the proposed experiments.

Finally, it should be pointed out that the proposed mechanism is preliminary and very debatable, especially the idea that a titanacyclobutane is formed which provides metal–alkyl $\sigma$-bonds. Certainly there might be other possibilities to account for the present results. We hope that theorists in the polymer area can provide some modeling work on these findings which, in turn, will stimulate experimental work to further explore the mechanisms of olefin polymerization.

## 5. Conclusions

In this paper we have described the application of SIDT-LV to studies of the gas-phase reactions of ethylene and propylene molecules with $Ti^+$ at thermal energies. The work provides a good example to illustrate that SIDT-LV is an effective tool for examining reactions such as the polymerization process which requires a large number of collisions between the injected ion and the reactant gas. The main conclusions drawn from the work can be summarized as follows:

(1) Bare $Ti^+$ exhibits a significant dehydrogenation reactivity toward ethylene and propylene. But the coordination of ligands can alter its dehydrogenation reactivity. In most of the cases, the addition of ligands will reduce and may even destroy the dehydrogenation reactivity of $Ti^+$, depending on the type of ligand.

(2) The reactions of $Ti^+$ with propylene terminate at the fourth step reactions, while reactions with ethylene are observed to continue up to at least the 20th step. On the basis of the various evidence presented, we believe the fact that as many as 20 ethylene molecules are able to attach onto a bare $Ti^+$ at room temperature indicates that an ethylene polymerization process induced by $Ti^+$ has occurred. Moreover, the ligands coordinated onto $Ti^+$ are observed to have a great impact on the ethylene polymerization.

(3) According to the point that ethylene has a much higher ionization potential than Ti, we rule out the possibility that the ethylene polymerization proceeds via a typical cationic polymerization mechanism. On the other hand, considering the role of titanium compounds in Ziegler–Natta catalysts and the existence of highly active cation-like catalysts in the condensed phase, we tend to believe that the gas-phase ethylene polymerization may follow a similar mechanism via which the condensed phase olefin polymerization catalyzed by Ziegler–Natta catalysts proceeds.

(4) By applying the basic ideas of Cossee's mechanism, we are able to establish a simple model to interpret the polymerization. The central point of our model is the formation of titanacyclobutane to provide metal–alky $\sigma$-bonds. This model states that after formation of titanacyclobutane, one of the coordinated ethylene molecules onto $Ti^+$ may undergo an interposition from the titanium ion to the alkyl group and create one vacant position for further coordination of ethylene molecules. Starting from the seventh ethylene molecule, the reactions of $Ti^+$ with ethylene involve only the coordination of an ethylene molecule onto $Ti^+$, and the ethylene then inserts into one of the metal–alkyl $\sigma$-bonds to form a larger titanacycloalkane. The reaction patterns continue expanding to form a larger and larger ethylene polymer.

**Acknowledgment.** Financial support by the Environment Protection Agency, Grant No. R-817437-01-0, and E. I. DuPont de Nemours and Co. through an unrestricted grant to The Pennsylvania State University are gratefully acknowledged.

**Registry No.** $C_2H_4$, 74-85-1; $C_3H_6$, 115-07-1; Ti, 7440-32-6.

(40) Guo, B. C.; Kerns, K. P.; Castleman, A. W., Jr., unpublished work.